

RESEARCH ARTICLE

The ocelli of Archaeognatha (Hexapoda): functional morphology, pigment migration and chemical nature of the reflective tapetum

Alexander Böhm* and Günther Pass

ABSTRACT

The ocelli of Archaeognatha, or jumping bristletails, differ from typical insect ocelli in shape and field of view. Although the shape of the lateral ocelli is highly variable among species, most Machiloidea have sole-shaped lateral ocelli beneath the compound eyes and a median ocellus that is oriented downward. This study investigated morphological and physiological aspects of the ocelli of *Machilis hrabei* and *Lepismachilis* spp. The light-reflecting ocellar tapetum in *M. hrabei* is made up of xanthine nanocrystals, as demonstrated by confocal Raman spectroscopy. Pigment granules in the photoreceptor cells move behind the tapetum in the dark-adapted state. Such a vertical pigment migration in combination with a tapetum has not been described for any insect ocellus so far. The pigment migration has a dynamic range of approximately 4 log units and is maximally sensitive to green light. Adaptation from darkness to bright light lasts over an hour, which is slow compared with the radial pupil mechanism in some dragonflies and locusts.

KEY WORDS: Vision, Raman spectroscopy, Nanocrystals, Spectral sensitivity, Jumping bristletail, Insect

INTRODUCTION

The structure and function of compound eyes in crustaceans and insects has been the subject of intense study over the last 120 years (e.g. Exner, 1891; Horridge, 1975; Strausfeld, 2005; Warrant, 2006; Land and Nilsson, 2012); however, comparatively little is known about the ocelli (for reviews, see Goodman, 1981; Mizunami, 1995; Krapp, 2009). Adult winged insects usually have three ocelli on the frons or vertex, a median ocellus and two lateral ones – not to be confused with stemmata, which are sometimes termed ‘lateral ocelli’ as well. From a morphological point of view, they are simple eyes in that they have a single lens. Ocelli are often more sensitive than compound eyes, because of a high convergence of photoreceptors onto secondary neurons, and the fewer neurons involved in processing the signals enable a faster response. The insight that the ocelli of some taxa are capable of any resolution at all is relatively recent (Schuppe and Hengstenberg, 1993; Stange et al., 2002; Berry et al., 2007a,b); nonetheless, the compound eyes outperform ocelli in this regard. The main functional role for ocelli in winged insects is likely flight stabilization (e.g. Taylor and Krapp, 2007), an idea that can also be implemented in aerial vehicles (Gremillion et al., 2014).

But what about insects that are weak flyers or unable to fly? Most beetles, for example, have no ocelli, and the two ocelli in the cockroach *Periplaneta* with a 2500:1 convergence ratio from receptors to second-order neurons are obviously adapted for light sensitivity (Toh and Sagara, 1984). Among the primarily wingless basal hexapods, Protura and Diplura are blind and possess neither ocelli nor compound eyes. The condition in Collembola is somewhat unusual in that there are up to six separate groups of 2 to 12 photoreceptor cells located beneath the unmodified head cuticle and epidermis, which are considered to be homologous to insect ocelli (Paulus, 1972).


Among hexapods, well-developed ocelli only occur in the ectognathan lineage, the oldest extant representatives of which are the jumping bristletails or Archaeognatha (Misof et al., 2014). These primarily wingless insects often feed on algae and lichens are generally found in rocky and moist habitats but also on trees. The anatomy of the ocelli of Archaeognatha was first described in two species of *Machilis* by Hesse (1901). He mentioned a reflecting tapetum with red-brown pigment behind it, while Hanström (1940) found brown-black pigment within whole photoreceptor cells of *Petrobius* (Machilidae). However, neither author considered that pigment migration might account for the observed differences, nor could they resolve the nature of the tapetum, which was described as connective tissue-like. Only Wygodzinsky (1941) and Paulus (1972) independently briefly noted that the ocelli of machilids turn white during dark adaptation, but did not provide further details. In her review of insect ocelli, Goodman (1981) stated: ‘The presence of pigment granules within the retinal cells is not compatible with the use of a reflecting tapetal layer, and the two are not found in association.’ In the present paper, we will clarify these obviously conflicting statements and describe for the first time a proximal–distal ocellar pigment migration in combination with a diffusely reflecting tapetum in representatives of the Archaeognatha.

Tapeta formed by reflecting crystalline deposits are quite common among animals, e.g. fish, cats, mollusks, spiders, crustaceans and insects (for a review, see Schwab et al., 2002). Although crystals of various substances can form multi-layer reflectors, the best studied is guanine (Land, 1972; Mueller and Labhart, 2010; Hirsch et al., 2015; Bossard et al., 2016; Jordan et al., 2014, 2012). Guanine or uric acid reflectors also cause color and color change phenomena in the integument of many animals, e.g. copepods (Chae et al., 1996), beetles (Caveney, 1971), spiders (Insausti and Casas, 2008) and chameleons (Teyssier et al., 2015).

The determination of the chemical nature of multilayer reflectors has been performed by chromatography, UV-Vis spectroscopy and histochemistry (Zyznar and Nicol, 1971; Chae et al., 1996; Mueller and Labhart, 2010). In the present analysis we demonstrate that Raman microspectrometry is likewise an

Department of Integrative Zoology, University of Vienna, Althanstr. 14, Vienna 1090, Austria.

*Author for correspondence (a.boehm@univie.ac.at)

 A.B., 0000-0001-7868-886X

appropriate method that even has considerable advantages over the others.

In Raman spectroscopy, the sample is illuminated with monochromatic light. A small fraction of the scattered light shows shifted frequencies because of interaction with vibrational modes characteristic of the sample (Raman and Krishnan, 1928). The benefits of confocal Raman spectroscopy in identifying the chemical nature of the tapetum crystals are twofold: the method is easy to use (simply place the sample on a slide) and the possible sub-micrometer spot size enables acquisition of spectra from very small sample areas. In our case, this is important because the tapetum cannot be mechanically separated from the pigment containing photoreceptor cells. Using a confocal Raman microscope, a suitable region can easily be targeted.

The goals of the present paper are twofold. First, to report our findings on the functional morphology of the ocelli in representatives of Archaeognatha. The results include a detailed description of the proximal–distal pigment migration in the photoreceptor cells that was found in all examined species. Second, to elucidate the chemical nature of the tapetum, its nanocrystals, their dimensions and arrangement. In addition, the data are discussed in light of several speculations on the biological role of the ocelli.

MATERIALS AND METHODS

Animals

Machilis hrabei Kratochvil 1945, *Lepismachilis y-signata* Kratochvil 1945 and *Lepismachilis notata* Stach 1919 were collected in the surroundings of Vienna, Austria, and kept indoors under the naturally prevailing light/dark cycle. *Acheta domesticus* (Linnaeus 1758) were bought in a local pet shop and stored frozen until they were dissected.

Histological sections

Standard histological techniques were employed (see Böhm et al., 2012) with the only exception that transmission electron microscopy (TEM) sections were contrasted with 2.5% gadolinium triacetate (Nakakoshi et al., 2011) instead of uranyl acetate. To examine single tapetum crystals, the dissected tissue was placed on the surface of distilled water. Mechanical stress and probably osmotic effects instantly cause the crystals to disperse out of the ruptured tissue. This allows them to be collected with Formvar-coated TEM grids. A Zeiss 902 or Libra 120 TEM was used to image the specimens.

Focal length determination

The lens of the median ocellus was dissected from the specimen in phosphate buffered saline and examined with a Leitz Dialux microscope without condenser using the ‘hanging drop’ method (Homann, 1924).

Raman microspectroscopy

Ocelli were dissected in deionized water and dried on an aluminum-coated slide. Raman spectra were acquired using a Horiba LabRAM HR Evolution confocal microspectrometer (Horiba Scientific, Edison, NJ, USA) with a 532 nm laser and 300 or 600 mm⁻¹ gratings. Spectra were baselined with the program Spekwin (version 1.72.0, <http://www.effemm2.de/spekwin>).

Pigment migration and spectral sensitivity

To record light adaptation dynamics, a dark-adapted animal (40 min) was placed under a Nikon SMZ 25 stereomicroscope and illuminated with bright white light (40 kLux). The computer program Fiji (Schindelin et al., 2012) was used to plot the mean pixel value of the ocelli in the recorded images against time.

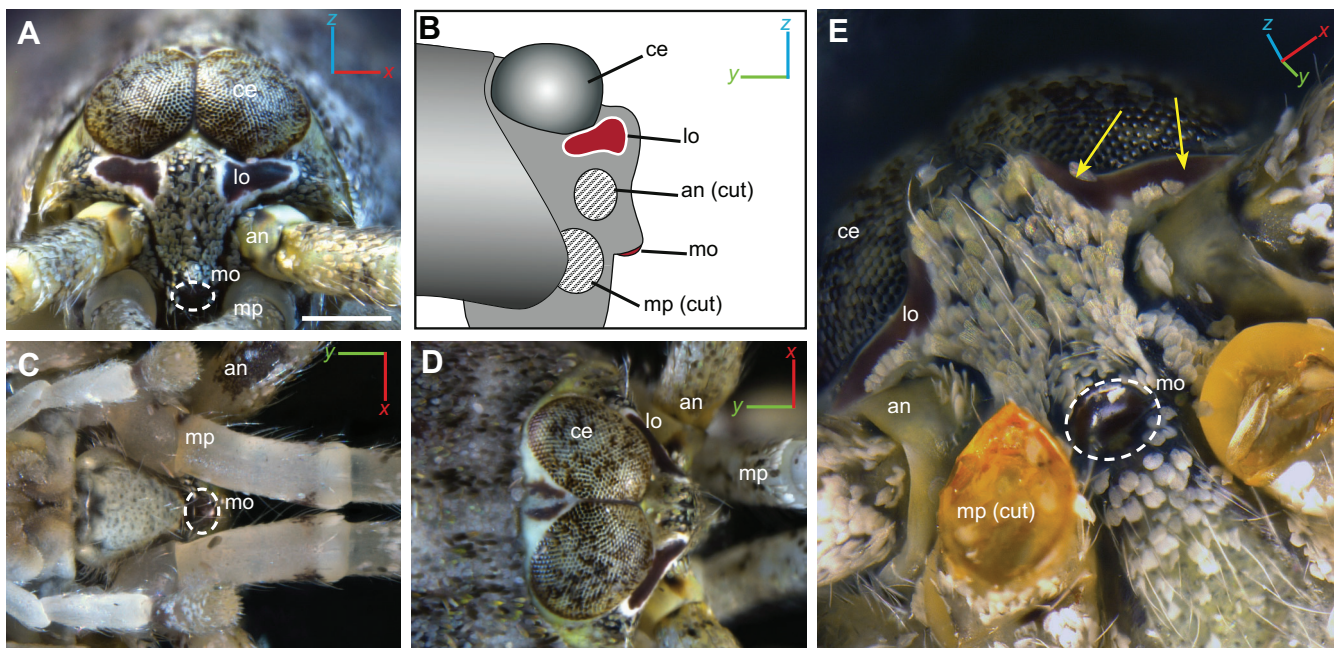


Fig. 1. General morphology of the ocelli in *Machilis hrabei*. (A–D) The lateral ocelli are situated immediately below the large compound eyes. The white border surrounding the reddish screening pigment is the only part of a tapetum that is visible in the depicted state of light adaptation. The median ocellus is located between the antennae and maxillary palps (removed); it has a lens-like cuticle and is oriented downward. Scale bar: 500 μ m. (E) Oblique ventral view of the lateral ocelli and the median ocellus (maxillary palps removed). Yellow arrows indicate that the curvature of the ocellus could contribute to discrimination of light incident from a frontal versus lateral direction. Abbreviations: an, antenna; ce, compound eye; lo, lateral ocellus; mo, median ocellus; mp, maxillary palpus.

In the other experiments, a Leica S6 E stereomicroscope was used, which was equipped with an 850 nm IR LED (infrared light emitting diode, ILH-IO01-85SL-SC201-WIR200) mounted onto one ocular and a camera mounted to the other ocular (MotiCam 2300; IR blocking filter replaced by an IR transparent longpass filter). Images were acquired with a custom μ Manager (<https://www.micro-manager.org>) script and data were plotted with LiveGraph (<http://www.live-graph.org>). LEDs driven by a custom constant current power supply were used as light sources (peak wavelengths: 365 nm: NCSU275T-U365; 460 ± 10 nm: LXML-PB01-0023; 530 ± 10 nm: LXML-PM01-0090; 590 ± 5 nm: LXML-PL01-0060; 630 ± 10 nm: LXML-PH01-0060). The light output from the LEDs was measured by placing a calibrated photodiode (FDS100, Thorlabs, Munich, Germany) under the microscope instead of the animal. The whole setup was shielded from ambient light and experiments were performed at 17°C between 18:00 h and 23:00 h.

To measure the spectral sensitivity, the intensity of the respective LED was adjusted until the same steady-state response (a certain mean pixel value) was achieved. The inverse of this intensity value is considered the sensitivity. Measurements were made from short to long wavelengths and in the reverse order to check for adaptation effects.

RESULTS

Morphology

In *M. hrabei*, the lateral ocelli are tilted 55 deg outward with respect to the sagittal plane and are oriented slightly upward with the median third being tilted outward only 20 deg. Hence the overall shape is concave and the median third covers a more lateral part of the visual field than the remaining ocellus. The median ocellus is located on an anterior prominence of the head capsule at the edge

between the frons and clypeus (Fig. 1). Its orientation is very unusual in that it is directed downward at an angle of approximately 65 deg (between the optical axis and a horizontal section plane; Fig. 1B). Moreover, the field of view is narrowed by the large maxillary palps and only a triangular window is left open by the shape and usual position of these palps. The cuticle of the lateral ocelli is only slightly curved and thus can be considered a transparent window (Fig. 2A,B), while the cuticle of the median ocellus is somewhat more lens-like (Figs 1E and 2C). Underneath the cuticle is a single-layered epidermis with small irregularly shaped nuclei (Fig. 2D). Slender processes from these epidermal cells extend between the photoreceptor cells. Each of the mostly X-shaped rhabdoms is formed by four photoreceptor cells with large, round nuclei that are located distally (Fig. 3A). Axons of the photoreceptor cells extend a short distance medially from the lateral ocelli, where they form a globular neuropil, adjacent to the brain, with dendrites of ‘downstream’ neurons (Hanström, 1940). Proximally, the photoreceptor cells run through holes within a tapetum consisting of cells with large elongated nuclei that are densely packed with xanthine crystals (Fig. 3C,E). One lateral ocellus has 105 ± 13 ($n=3$) such holes in its tapetum, which equals approximately 420 photoreceptor cells per ocellus because the photoreceptor cells run through the holes in groups of four (Fig. 3B).

Optics of the ocelli

Many of the concepts used to describe the sensitivity and resolution of animal eyes assume a circular aperture and an image that is focused on the retina (Land, 1981). As these two assumptions are clearly violated in the lateral ocelli, we focused our attention on the optical properties of the median ocellus of *M. hrabei*. The back focal distance (i.e. the distance from the back surface of the lens to

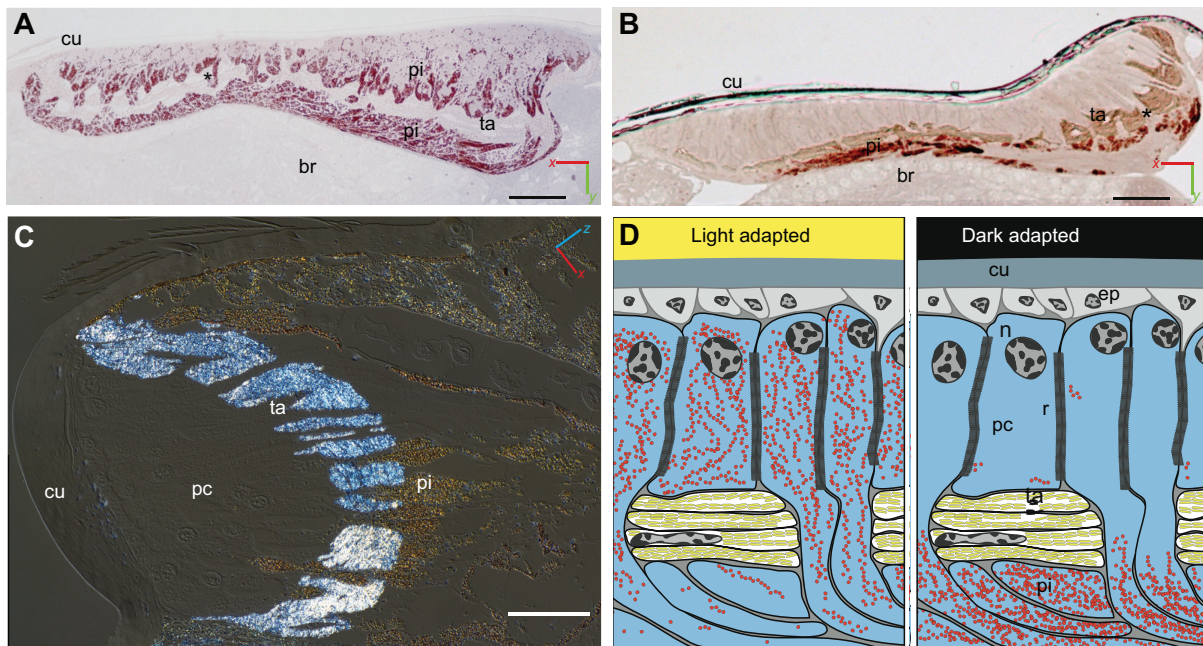


Fig. 2. Light/dark adaptation and ultrastructure of the lateral ocellus. (A) Partially light-adapted lateral ocellus of *Lepismachilis y-signata* showing screening pigment in front and behind the tapetum (unstained horizontal section, 1 μ m). (B) Dark-adapted lateral ocellus of *L. y-signata* with all pigment located behind the tapetum (unstained horizontal section, 3 μ m). (C) Unstained semi-thin section of the median ocellus (differential interference contrast with almost crossed polarizers). Because of their birefringence, the crystals in the tapetum appear bright white or blue, depending on their orientation. (D) Schematic summary of A–C showing an ocellar region adapted to light and darkness. Abbreviations: br, brain; cu, cuticle; ep, epidermis; n, nucleus; pc, photoreceptor cells; pi, pigment; r, rhabdom; ta, tapetum. Scale bars: (A,B) 50 μ m, (C) 25 μ m.

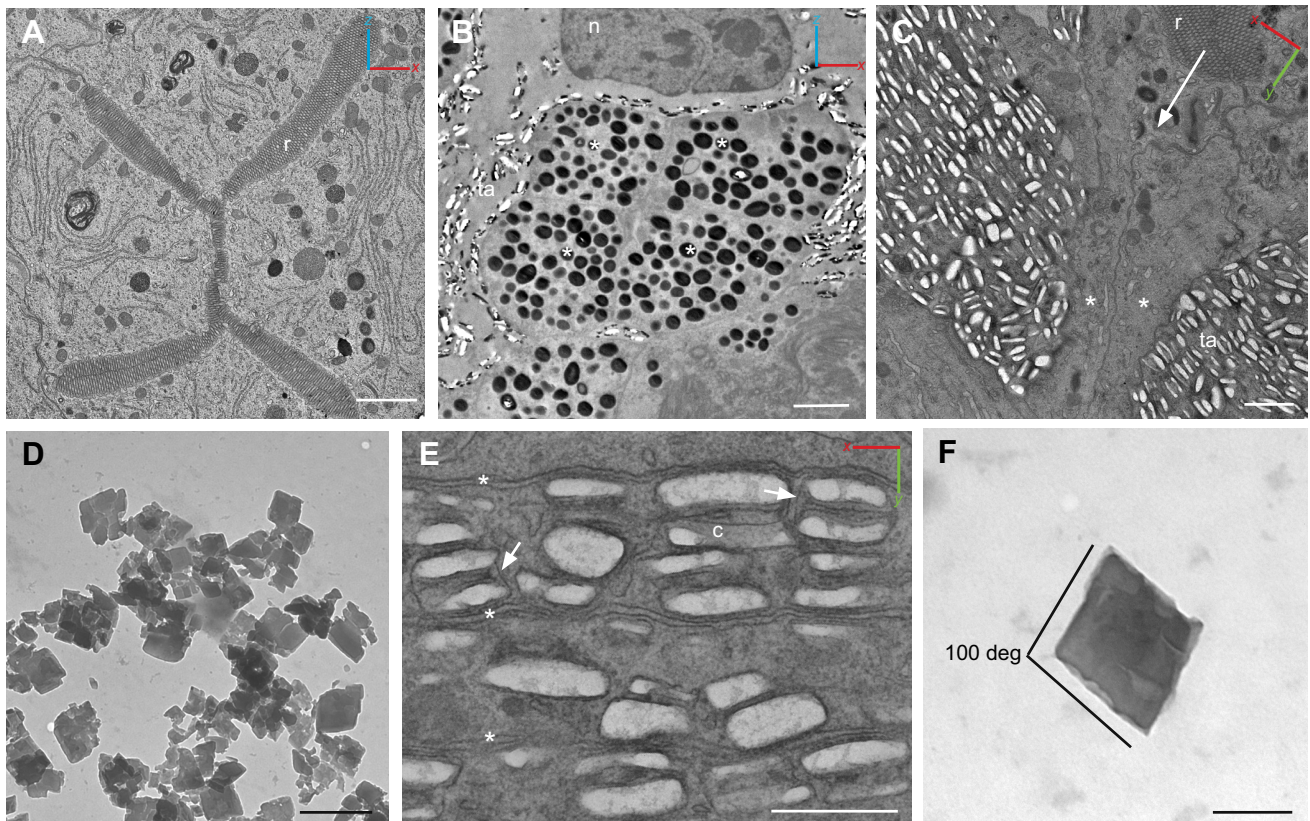


Fig. 3. Ultrastructure of the lateral ocellus. (A) Typical X-shaped rhabdom made up of four photoreceptor cells in a dark-adapted lateral ocellus. For a larger version of this image, see Fig. S1A. (B) Cross-section showing groups of four retinula cells with internal pigment (asterisks) at the level of the tapetum. (C) Horizontal section through a lateral ocellus showing preferential orientation of the flat face of the tapetum crystals perpendicular to incoming light rays (arrow) normal to the cuticle; two photoreceptor cells penetrating the tapetum are marked by asterisks. Note that crystals frequently fall out of ultrathin sections or become dissolved. (D) Group of crystals of the tapetum collected on a Formvar-coated TEM grid. The crystals show various degrees of damage, which could be caused by partial dissolution or mechanical damage during preparation. Nonetheless, many of them still exhibit a recognizable rhomboid geometry. (E) Individual crystals appear to be enclosed by a membrane, and typically two tapetum crystals are packaged together by an additional membrane (arrows). Most of the elongated tapetum cells contain four layers of crystals, i.e. two layers of two-by-two packed crystals (cell membranes of the three tapetum cells in the image marked by asterisks). (F) Single rhomboid tapetum crystal. (A,C–F) *Machilis hrabei*. (B) *Lepismachilis y-signata*. Abbreviations: c, crystal; n, nucleus; r, rhabdom; ta, tapetum. Scale bars: (A,B) 2000 nm, (C,D) 1000 nm, (E) 500 nm, (F) 200 nm.

the image) of dissected median ocellus lenses measured by the hanging drop method was $203 \pm 67 \mu\text{m}$ ($n=4$). The rather high variation is attributed to different body size of the animals and to the difficulty of orienting the optical axis of the dissected lens perfectly parallel to that of the microscope.

The reflection spectrum of the tapetum or the amount of specular versus diffuse reflection has yet to be measured. When visually examining dark-adapted ocelli that are illuminated by incident light from various angles, the reflection seems to be mainly diffuse. However, the partly ordered tapetum suggests that the reflection could have diffuse and specular components. In the following optical model, we assume full specular reflection, as that is the only case that can be readily calculated and, while not observed so far, it could occur naturally in species with a slightly more ordered crystal arrangement. In addition, we qualitatively discuss the effect of a diffuse reflection.

The position of the focal point of the lens–mirror system (Fig. 4) was determined using the ‘vergence method’ of geometrical optics (e.g. Meyer-Arendt, 1995). The initial convergence of a distant point source, C_0 , is zero and the subsequent convergences C_i were found by considering the optical powers of the refracting (P_0 , P_1) and reflecting (P_2) interfaces of radii r_j and adding terms for the

distances t_k between them:

$$\begin{aligned}
 C_0 &= 0 \\
 C_1 &= P_0 = \frac{n_1 - n_0}{r_0} \\
 C_2 &= \frac{n_1 C_1}{n_1 - t_0 C_1} \\
 C_3 &= C_2 + P_1 = C_2 + \frac{n_2 - n_1}{r_1} \\
 C_4 &= \frac{n_2 C_3}{n_2 - t_1 C_3} \\
 C_5 &= C_4 + P_2 = C_4 - \frac{2n_2}{r_2}.
 \end{aligned} \tag{1}$$

The distance of the focal point from the back surface of the lens was $t_1 - (n_2/C_5) = 45 \mu\text{m}$ and, after adding half the thickness of the lens, this can be taken as approximation of the focal length $f = 54 \mu\text{m}$ of a single thin lens that has the same effect as the calculated combination (values used in the calculation are as follows, where

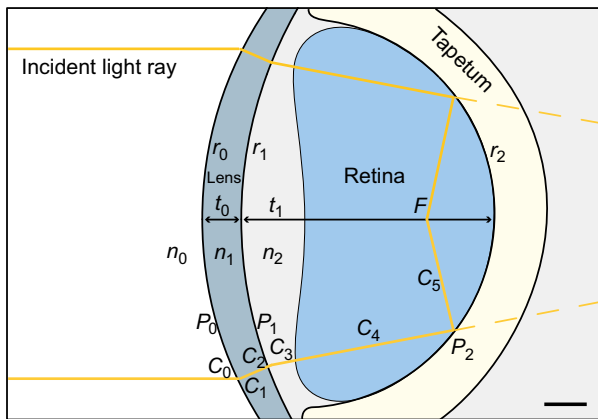


Fig. 4. Optical model of the median ocellus. Incident parallel rays (yellow) are refracted by the cuticular lens, pass the retina and are focused by the tapetum within the retina (focal point F). The dashed rays indicate that the focal length of the system would be much longer without a tapetum. This model assumes full specular reflection while the tapetum of *Machilis hrabei* likely shows mixed reflection. Symbols defined in the Results. Scale bar: 20 μm .

n are refractive indices, lengths in μm : $n_0=1.0$, $n_1=1.5$, $n_2=1.33$, $t_0=18$, $t_1=65$, $r_0=57$, $r_1=100$ and $r_2=-50$. The back focal distance of the lens alone is given by $n_2/C_3=164 \mu\text{m}$. Under the simplifying assumption of a circular aperture with diameter $A=100 \mu\text{m}$, this gives a very low F number of $f/A=0.54$. The rhabdoms have a cross-sectional area of $37.9\pm23.3 \mu\text{m}^2$ ($n=53$, ratio of rhabdom to retinal area $p_r=0.17$) which corresponds to a circle with diameter $d=6.9 \mu\text{m}$. For the rhabdomere absorption coefficient k , the value obtained for lobster (Warrant and Nilsson, 1998) is assumed, and the rhabdomere length l is 40 μm . Now the sensitivity of the ocellus for an extended scene illuminated by white light can be estimated as $S = \left(\frac{\pi}{4}\right)^2 \left(\frac{Ad}{f}\right)^2 P = 10.5 \mu\text{m}^2 \text{sr}$ (Warrant and Nilsson, 1998).

In this formula, $P = \left(\frac{kl}{2.3 + kl}\right)$ stands for the fraction of light absorbed by photopigments within the rhabdoms. This value can be corrected, accounting for the fact that rhabdoms only cover a fraction of the retina, by multiplication with p_r . In the dark-adapted state, light that is not absorbed in the first pass is reflected back through the retina. This effect can be approximated by multiplication of S by $p_r + p_r(1-P) = p_r(2-P)$. According to Speiser and Johnsen (2008), this correction factor would only be $1-P$ because they assume that the absorption of unfocused light in the first pass decreases sensitivity. We suggest that the light absorbed in the first pass through the retina, which is pre-focused by the cuticular lens, increases sensitivity while decreasing resolution. So the final sensitivities in the light- and dark-adapted states become $S_{\text{light}} = p_r S = 1.8 \mu\text{m}^2 \text{sr}$ and $S_{\text{dark}} = p_r(2-P)S = 3.4 \mu\text{m}^2 \text{sr}$, respectively.

The back focal distance of the slightly curved surface of the lateral ocellus calculated as above was 831 μm ($r_0=200 \mu\text{m}$, $r_1=207 \mu\text{m}$, other parameters as for the median ocellus). This is approximately 15 times the depth of the lateral ocellus, thus the refracting interface behaves essentially like a flat light window. The curvature in the tapetum is convex in the central region, while in the median and lateral parts it is concave (Fig. 2A,B).

Tapetum crystal arrangement

The individual crystals of the tapetum are small rhomboid platelets of $440\pm111 \text{ nm}$ edge length and an obtuse angle of $99.1\pm4.8 \text{ deg}$ as

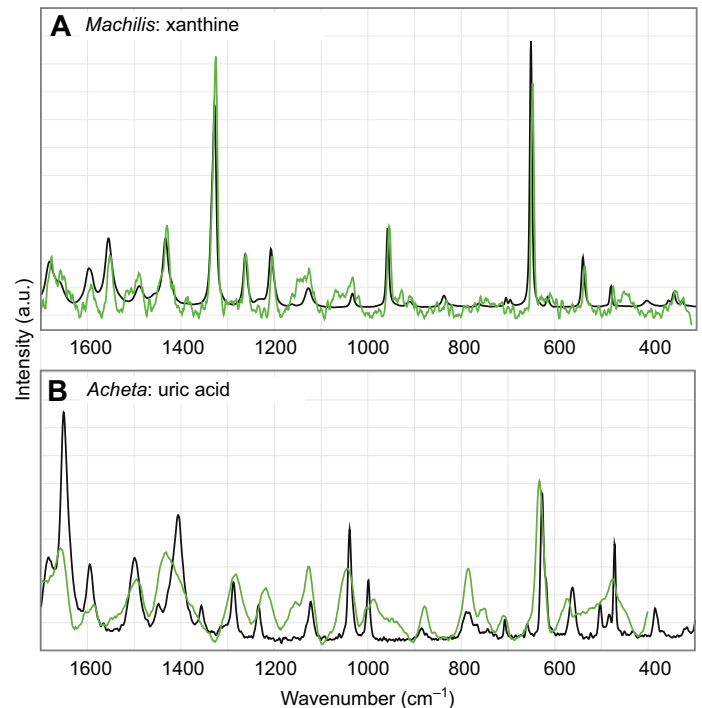


Fig. 5. Raman spectroscopy of the tapetum. (A) Raman spectrum of the tapetum of a lateral ocellus of *Machilis hrabei* (green line) and reference spectrum for pure xanthine (black line). (B) Raman spectra of *Acheta domesticus* ocellar tapetum (green line) and pure uric acid (black line).

measured from free crystals on a Formvar film ($n=20$; Fig. 3D,F). Although the solubility of xanthine in water (0.069 g l^{-1} at 16°C O'Neil, 2006) and alcohol is low, the crystals are almost always lost during ultrathin section preparation. In favorable sections with at least partially remaining crystals, the resulting gaps are informative. These gaps are $56\pm24 \text{ nm}$ ($n=78$) wide and $363\pm122 \text{ nm}$ ($n=122$) long. The crystals often occur in groups of two crystals that have the same orientation and a smaller distance between them ($70\pm19 \text{ nm}$, $n=38$) than between two adjacent crystals that are not necessarily from the same 'package' ($100\pm50 \text{ nm}$, $n=20$). These packages, as well as the individual crystals, are enclosed by a membrane and typically two such packages are stacked in a tapetum cell in the direction of incident light (Fig. 3E). The crystals are preferentially orientated with their largest face parallel to the cuticle of the ocelli, and the standard deviation of the angle at which the crystals are oriented in the tapetum was determined to be 22 deg (from seven horizontal sections). The thickness of the tapetum lies between 12 to 30 μm and consists of a stack of 20 to 30 crystal layers.

Confocal Raman spectroscopy

Raman microspectroscopy of the tapetum of *M. hrabei* yielded spectra (Fig. 5A) with a close correspondence of peak positions and intensities to those of xanthine (<http://www.sigmaaldrich.com/spectra/rair/RAIR000286.PDF>, #X7375). For comparison, the white tapetum material in the ocelli of *Acheta domesticus*, which contain no pigment, was likewise examined with Raman spectroscopy (Fig. 5B). The spectrum agrees with that of uric acid (<http://www.sigmaaldrich.com/spectra/rair/RAIR002210.PDF>, #U2625), although not as well as in the xanthine case. The red pigment of *M. hrabei* ocelli has a spectrum with three poorly separated peaks at 1330, 1487 and 1625 cm^{-1} (Fig. 6).

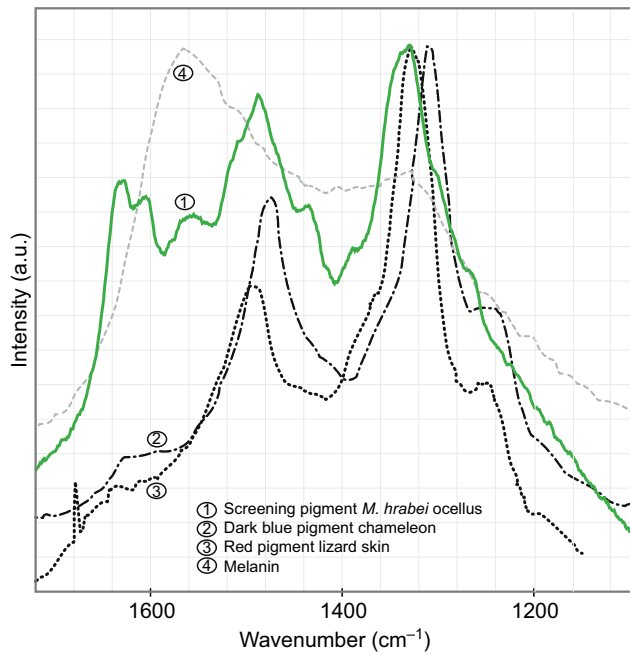


Fig. 6. Screening pigment Raman spectrum. The Raman spectrum of the red pigment in the ocelli of *Machilis hrabei* (green line) has three confluent peaks at 1330, 1487 and 1625 cm^{-1} . Raman spectra of pigments from dark blue skin melanophores of panther chameleons (Teyssier et al., 2015) and red skin erythrophores of the lizard *Phelsuma lineata* (Saenko et al., 2013) exhibit two similar peaks, but the region around 1600 cm^{-1} is different. The spectrum of melanin from dark-brown chameleon skin melanophores (Teyssier et al., 2015) only shows a single broad peak around 1580 cm^{-1} .

Dynamics and spectral sensitivity of pigment migration

In light-adapted *M. hrabei*, large amounts of red pigment granules in the retinula cells are located in front of the tapetum but migrate completely behind it upon dark adaptation (Fig. 2A,B,D). The tapetum is visible as a white border around the lateral ocellus in light-adapted *M. hrabei* but not in the investigated species of *Lepismachilis*.

The mechanism that triggers the pigment migration is maximally sensitive to green light (Fig. 7A). Because of the limited number of LED wavelengths and comparatively high spectral half-width, the wavelength of peak sensitivity can only be determined as 530 ± 30 nm. The sensitivity curve falls off more steeply on the long-wavelength side of the peak than in the blue–UV region.

The pigment migration response is not ‘all or nothing’ but reaches a steady state corresponding to the irradiance of the ocellus. For the lateral ocellus of *M. hrabei*, this response follows a sigmoid function (Fig. 7B) and the dynamic range spans approximately four decades. The temporal dynamics of the transition from the dark- to the light-adapted state likewise resulted in a sigmoid curve when plotting the reflectance of the ocellus over time after switching on the light (Fig. 7C–E, Movie 1). Full adaptation to bright light requires approximately 1.5 h and is comparably fast in *M. hrabei* and *Lepismachilis notata*.

DISCUSSION

Sensitivity and resolution

A striking feature in machilids is the oddly shaped lateral ocelli. While sole-shaped lateral ocelli are probably a plesiomorphic character for Machiloidea, various other shapes and positions occur (e.g. *Dilta*: round, lateral; *Trigoniophthalmus*: tear shaped, median;

Machilinus: round, lateral) (Sturm and Machida, 2001). With our present knowledge on the biology of Archaeognatha, it is not possible to clearly correlate the shape of the lateral ocelli with any particular lifestyle, but a reasonable assumption is that the ocellus area is enlarged to enhance photon capture in dark environments.

The only potential for resolution in the lateral ocelli can be derived from the curvature of the lateral ocellus, because light incident from lateral (yellow arrows in Fig. 1E) will produce higher irradiance in the median part, whereas frontal light will lead to higher irradiance in the lateral part. The acceptance angle of a rhabdom, $\alpha = 2 \cos^{-1} \left(\frac{n_o}{n_{rh}} \right)$, depends on the refractive indices of the rhabdom, n_{rh} , and of the outer medium, n_o (Miller, 1979). This will, together with shading effects, enhance resolution of the lateral ocelli in the light-adapted state because screening pigment raises n_o , an effect observed in various compound eyes (Miller, 1979). However, this increase in resolution will be rather small given the weak ocellus lens, and we hypothesize that the main function of the pigment migration is to attenuate intense daylight.

Most Archaeognatha have black, brown or red pigment in their ocelli; only some Meinertellidae, especially *Machilinus* sp., seemingly lack any pigment (Sturm and Machida, 2001; Sturm and Smith, 1993). Remarkably, *Machilinus* species are active during the day (Sturm, 1997), in contrast to almost all other Archaeognatha. The presence of black ocelli in members of the subgenus *Protomachilinus* could be indicative of an adaptation toward activity in a darker environment (Sturm, 1997). Insects that face strongly changing light intensities during their activity periods probably need a way to protect their sensitive photoreceptors from overexposure. Other insects that are active under more constant illumination conditions, such as *Periplaneta* (darkness) and *Locusta* (diurnal), often lack ocellar pigment and their ocellar photoreceptors could be adapted to these specific light intensities.

The median ocellus could have some spatial resolution in the dark-adapted state if the reflection from the tapetum were specular. Nonetheless, the incident and reflected light would first pass through the ‘wrong’ rhabdoms until it finally reached the focal point. This would be a detrimental condition in terms of resolution, as noted for other eyes with reflectors by Land and Nilsson (2012). The sensitivity of the median ocellus clearly lies above the typical values for apposition compound eyes in Archaeognatha. For comparison, the compound eye of a bee has a calculated sensitivity (Land, 1981) that is approximately 10 times lower than the estimate we obtained for the dark-adapted median ocellus of *M. hrabei*.

To summarize, we hypothesize that the ocelli of Archaeognatha have reasonable sensitivity, permitting crepuscular activity, yet very poor resolution. The lateral ocelli have a larger field of view and a potential for some resolution because of their shape. Mizunami (1995) suggested that the ancestral insect ocellar system (e.g. Odonata) had both bi- and trisynaptic pathways and was concerned with optimization of both speed and sensitivity. Given the condition found in Archaeognatha [fast jumping/gliding behaviors (see below), adjustable sensitivity], we anticipate that such a neural organization could also be present in Archaeognatha.

Tapetum structure

In the past few years, theoretical and experimental interest in guanine multilayer reflectors was very high because of potential biomimetic applications (Bossard et al., 2016; Iwasaka et al., 2016; Hirsch et al., 2015; del Barco et al., 2015; Gur et al., 2015a,b, 2013; Jordan et al., 2014, 2012; Oaki et al., 2012; Levy-Lior et al., 2008).

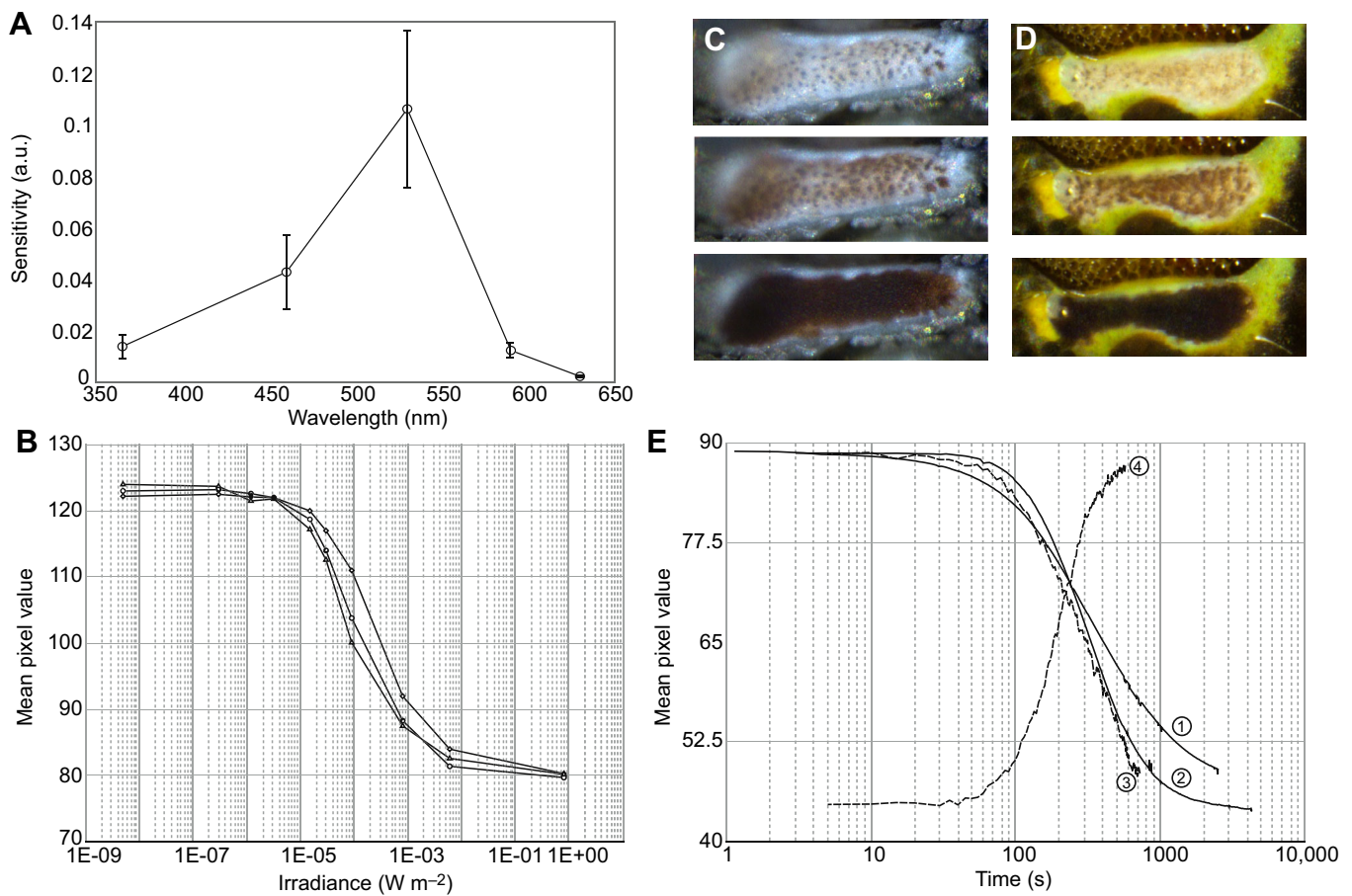


Fig. 7. Pigment migration in the lateral ocellus. (A) The pigment migration reaction in the lateral ocellus of *Machilis hrabei* is maximally sensitive to green light and the sensitivity falls off faster in the red than in the blue–UV region of the spectrum ($n=8$: 5 females, 2 males, 1 juvenile; bars indicate s.e.m.). (B) Steady-state pigment migration response to a given irradiance in the lateral ocellus of *M. hrabei*. (C,D) Snapshots during three stages of light adaptation in the lateral ocelli of *M. hrabei* (C) and *Lepismachilis notata* (D). (E) Pigment migration dynamics after 40 min of dark adaptation (bright white light illumination; curve 1: *L. notata*; curves 2, 3: *M. hrabei*). During dark adaptation, the migration dynamics also follow a sigmoid time course (darkness after 40 min of white light; curve 4). Curves 1 and 2 were measured from the same data that were used for Movie 1; curves 3 and 4 show the extent of pigment migration measured in the infrared region.

These recent theoretical works have taken disorder into account, i.e. variation in the thickness of crystal and inter-crystal layers; however, in more diffuse reflectors, the three degrees of rotational freedom of the crystals needs to be addressed as well.

No clear-cut evolutionary pattern of tapetum types in hexapod ocelli is discernible. Reflective crystal tapeta are relatively common in insect ocelli, for example, in cicadas (Ribi and Zeil, 2015), dobsonflies (Megaloptera), odonates, cockroaches and locusts (Goodman, 1981). Tracheolar tapeta in the ocelli are reported to occur in Diptera (Goodman, 1970), Hymenoptera (Somanathan et al., 2009) and tentatively also Trichoptera (Hallberg and Hagberg, 1986). Thus, despite the present scarcity of data, the presence of tracheolar tapeta in ocelli could be an evolutionary novelty of certain Holometabola. In the hemimetabolous Odonata, tracheoles between the photoreceptor cells seem to optically insulate them from each other to some degree (Stange et al., 2002).

The reflective tapetum of crustacean nauplius eyes is in some groups crystalline, e.g. in ostracods (Meyer-Rochow, 1999; Andersson and Nilsson, 1981) and copepods (Fahrenbach, 1964), yet in ‘Conchostraca’, round granules occur that are comparable to those in crustacean compound eyes (Reimann and Richter, 2007). It may be hypothesized that vesicles filled with high refractive index substances are an evolutionary precursor to crystalline tapeta

because the crystals also form inside membranous vesicles (Fig. 3E).

Tapetum crystal and screening pigment chemistry

Several reviews and textbooks claim that the tapetum is formed of urate crystals in *Schistocerca* (Goodman, 1970), *Periplaneta* (Goodman, 1981) and in the ‘typical insect ocellus’ (Chapman, 1998; Lancaster and Downes, 2013; Klowden, 2013). However, as rigorous tests demonstrating the chemical nature of the tapetum crystals have rarely been performed, our finding of xanthine, which is very similar to both guanine and uric acid, might not be uncommon. In crustaceans, high amounts of xanthine were found in mantis shrimp eye extract, but it was not determined whether it occurs specifically in the tapetum (Zyznar and Nicol, 1971). In the same study, 19 malacostracan eyes were examined for purines and pteridines, but the reflecting layers were separately analyzed only in *Penaeus setiferus*. In this species, the main component found was isoxanthopterin, and it was concluded that it could cause the observed reflection. In *Homarus*, reflective layers in the compound eye contain uric acid, xanthine, hypoxanthine, xanthopterin and an unidentified pteridine, but it is unclear which causes the reflection (Kleinholz, 1959). Kleinholz (1959) also found that the reflecting layer in *Limulus* eyes mainly contains guanine.

Xanthine is known to be created either from guanine by guanine deaminase, from hypoxanthine by xanthine oxidoreductase or from xanthosine by purine nucleoside phosphorylase, and it is converted to urate by xanthine oxidase (KEGG pathway ko:00230; Kanehisa et al., 2014). Some lichens inhibit xanthine oxidase (Behera et al., 2003), which might cause elevated xanthine levels in animals consuming them. Although this has only been reported for tropical lichen species, it may bear some significance as the investigated Archaeognatha were fed with lichens. The same 100 deg angle as in archaeognathan xanthine crystals was found in the monoclinic unit cell of the tetrahydrate sodium salt of xanthine (Mizuno et al., 1969). It is thus plausible that the flat face of the crystals, which is oriented toward the incident light, is the (010) face of monoclinic crystals. Nonetheless, further investigation, e.g. using electron diffraction, is needed to verify this observation because the crystals are also compatible with the triclinic or orthorhombic systems.

The Raman spectrum of the red pigment (Fig. 6) encountered in the ocelli of *M. hrabei* is similar to the unidentified blue pigment spectra in chameleons (Teyssier et al., 2015) and the red and green pigment spectra in lizards (Saenko et al., 2013). They, in turn, resemble the Raman spectra of xanthopterin and isoxanthopterin (Saenko et al., 2013; Feng et al., 2001). There is little correspondence with the Raman spectra of melanin, carotene and the simulated spectrum of the ommochrome ommin (Hsiung et al., 2015).

Pigment migration

Migration of pigment, in the shape of a pupil formed by specialized cells between the lens and the receptor cells, has been described for the ocelli of dragonflies (Stavenga et al., 1979) and locusts (Wilson, 1975). Goodman (1981) also lists bees as having such an iris, but does not provide further details. In Heteroptera, vertical migration of pigment occurs in the photoreceptor cells of the tapetum-less ocelli of *Rhodnius* (Goodman, 1981) and *Triatoma* (Insausti and Lazzari, 2002). In Odonata, the retinula cells are ensheathed by tapetal cells whose nuclei are located distally, whereas the nuclei of the retinula cells are situated proximally above a layer of pigment cells (Ruck and Edwards, 1964). The retinula cells do not contain pigment granules as observed in Archaeognatha.

The spectral sensitivity (i.e. the action spectrum) of the pigment migration in ocelli has, to our knowledge, only been determined for two species of Odonata (Stavenga et al., 1979). Regarding compound eyes in several insects (Stavenga, 1979) and the crustaceans *Procambarus* (Olivo and Chrismer, 1980) and *Gonodactylus* (Cronin and King, 1989), it was shown that the action spectrum of the pigment migration closely matches the photoreceptor response spectrum. Only putative long-wavelength-sensitive opsin was found to be expressed in head regions containing ocelli of various odonates in a transcriptome sequencing study (Futahashi et al., 2015). Interestingly, the response to UV stimuli was twofold to ninefold higher than to green stimuli in the dragonfly *Hemicordulia tau* (van Kleef et al., 2005). In locusts, Wilson (1978) found evidence for UV and green visual pigment.

Apart from light, temperature is another factor that profoundly influences pigment migration in compound eyes of insects (Nordström and Warrant, 2000) and crustaceans (King and Cronin, 1994a,b). In the latter, microtubules are believed to mediate the granule transport (King and Cronin, 1994b). In the bug *Triatoma*, neither temperature nor circadian rhythm has an effect on the pigment position inside the ocellar retinula cells (Lazzari et al., 2011). It seems that pigment migration in the pigment cells of insect compound eyes is not neuronally controlled but rather is modulated by catecholamines (Hamdorf et al., 1989). Wilson

(1975) found that the adaptation mechanism for the radial pupil in some locusts clearly depends neither on the circadian rhythm nor on neural or hormonal control. It is not known whether these pupil cells are photosensitive themselves or are electrically or chemically influenced by the nearby photoreceptor cells.

Functional role of the ocelli

Among arthropods, and especially insects, the ocelli of Archaeognatha are unique in that the visual field of their median ocellus is oriented toward the ground. A possible function of the median ocellus could be to sense the optical properties of the surface the animals walk upon, in order to select a spot that provides optimal camouflage. Blending with their environment is obviously vital for Archaeognatha as most of them have a cryptic coloration over the entire body, including the compound eyes. The median ocellus could also be useful for spatial orientation because it faces the sky when the animals crawl upside down on tree limbs or peak out from the undersides of rock slabs, where they often rest.

Ocelli apparently only play a minor role in circadian entrainment (Saunders, 1976; Rieger et al., 2003; Tomioka and Abdelsalam, 2004), although nothing is known about this topic in Archaeognatha. Likewise, there is no information on whether the ocelli in Archaeognatha are involved with navigational behaviors, as in ants (Schwarz et al., 2011a,b).

Polarization sensitivity has been reported for few hymenopteran ocelli (for a review, see Zeil et al., 2014). It requires that the microvilli are parallel and the rhabdomere is as straight as possible (Ribi et al., 2011). In the X-shaped rhabdomes of archaeognathan ocelli, parts of two almost perpendicular arms are formed by each of the four receptor cells (Fig. S1). Thus no or very low net polarization sensitivity can be expected (Waterman, 1981).

The main function of well-developed ocelli in winged insects is flight stabilization (Wilson, 1978; Mizunami, 1995; Krapp, 2009). Although Archaeognatha cannot fly, they jump (Evans, 1975), and some of them achieve a directed aerial descent from trees (Yanoviak et al., 2009). When dropped from a tree, they glide back to the trunk, which most likely indicates a visually guided behavior. The relative importance of the compound eyes versus the ocelli has not been investigated in this behavior so far. Dudley and Yanoviak (2011) proposed an eight-step scenario for the evolution of flight, the first five of which Archaeognatha fulfill. Steps one to three are residence on elevated substrates, jumping/falling and aerial righting/landing reflexes. Therefore, it is possible that the ocelli already started to play an important role during the aerial endeavors of the primarily wingless Archaeognatha by providing faster feedback and higher sensitivity in low light conditions compared with compound eyes. It would be a highly interesting topic for future studies to determine the relative contribution of the ocelli and the compound eyes to the jumping and gliding behaviors of Archaeognatha.

Acknowledgements

We thank Markus Schmid (Department of Microbial Ecology, University of Vienna) for enabling the Raman measurements, the Core Facility Cell Imaging and Ultrastructure Research (University of Vienna) for access to the TEM, John Plant for checking the English and two anonymous reviewers for their constructive comments.

Competing interests

The authors declare no competing or financial interests.

Author contributions

A.B. conceived the study, conducted the experiments and drafted the manuscript. G.P. contributed to the manuscript.

Funding

The Austrian Science Fund FWF provided financial support (P 23251-B17).

Supplementary information

Supplementary information available online at

<http://jeb.biologists.org/lookup/doi/10.1242/jeb.141275.supplemental>

References

- Andersson, A. and Nilsson, D.-E. (1981). Fine structure and optical properties of an ostracode (Crustacea) nauplius eye. *Protoplasma* **107**, 361–374.
- Behera, B. C., Adawadkar, B. and Makhija, U. (2003). Inhibitory activity of xanthine oxidase and superoxide-scavenging activity in some taxa of the lichen family Graphidaceae. *Phytomedicine* **10**, 536–543.
- Berry, R., van Kleef, J. and Stange, G. (2007a). The mapping of visual space by dragonfly lateral ocelli. *J. Comp. Physiol. A Neuroethol. Sens. Neural. Behav. Physiol.* **193**, 495–513.
- Berry, R. P., Warrant, E. J. and Stange, G. (2007b). Form vision in the insect dorsal ocelli: an anatomical and optical analysis of the locust ocelli. *Vision Res.* **47**, 1382–1393.
- Böhm, A., Szucsich, N. U. and Pass, G. (2012). Brain anatomy in Diplura (Hexapoda). *Front. Zool.* **9**, 26.
- Bossard, J. A., Lin, L. and Werner, D. H. (2016). Evolving random fractal cantor superlattices for the infrared using a genetic algorithm. *J. R. Soc. Interface* **13**, 20150975.
- Caveney, S. (1971). Cuticle reflectivity and optical activity in scarab beetles: the role of uric acid. *Proc. R. Soc. Lond. B Biol. Sci.* **178**, 205–225.
- Chae, J., Kita-Tsukamoto, K., Nishida, S. and Ohwada, K. (1996). Chemical composition of the integumental reflecting platelets in the iridescent copepods of the family Sapphirinidae (Poecilostomatoida). *J. Crust. Biol.* **16**, 20–23.
- Chapman, R. F. (1998). *The Insects: Structure and Function*. Cambridge: Cambridge University Press.
- Cronin, T. W. and King, C. A. (1989). Spectral sensitivity of vision in the mantis shrimp, *Gonodactylus oerstedii*, determined using noninvasive optical techniques. *Biol. Bull.* **176**, 308–316.
- del Barco, O., Gasparian, V. and Gevorgian, Z. (2015). Localization length calculations in alternating metamaterial-birefringent disordered layered stacks. *Phys. Rev. A* **91**, 063822.
- Dudley, R. and Yanoviak, S. P. (2011). Animal aloft: the origins of aerial behavior and flight. *Integr. Comp. Biol.* **51**, 926–936.
- Evans, M. E. G. (1975). The jump of *Petrobius* (Thysanura, Machilidae). *J. Zool. Lond.* **176**, 49–65.
- Exner, S. (1891). *Die Physiologie der facettierten Augen von Krebsen und Insekten*. Leipzig und Wien: Franz Deuticke.
- Fahrenbach, W. H. (1964). The fine structure of a nauplius eye. *Z. Zellforsch.* **62**, 182–197.
- Feng, Z., Liang, C., Li, M., Chen, J. and Li, C. (2001). Surface-enhanced Raman scattering of xanthopterin adsorbed on colloidal silver. *J. Raman Spectr.* **32**, 1004–1007.
- Futahashi, R., Kawahara-Miki, R., Kinoshita, M., Yoshitake, K., Yajima, S., Arikawa, K. and Fukatsu, T. (2015). Extraordinary diversity of visual opsin genes in dragonflies. *Proc. Natl. Acad. Sci. USA* **112**, E1247–E1256.
- Goodman, L. J. (1970). The structure and function of the insect dorsal ocellus. *Adv. Insect Physiol.* **7**, 97–195.
- Goodman, L. (1981). Organisation and physiology of the insect dorsal ocellar system. In *Comparative Physiology and Evolution of Vision in Invertebrates. C: Invertebrate Visual Centers and Behavior II*, Vol. VII/6C of Handbook of Sensory Physiology (ed. H. Autrum), pp. 201–286. Berlin: Springer.
- Gremillion, G., Humbert, J. S. and Krapp, H. G. (2014). Bio-inspired modeling and implementation of the ocelli visual system of flying insects. *Biol. Cybern.* **108**, 735–746.
- Gur, D., Politi, Y., Sivan, B., Fratzl, P., Weiner, S. and Addadi, L. (2013). Guanine-based photonic crystals in fish scales form from an amorphous precursor. *Angew. Chem. Int. Ed. Engl.* **52**, 388–391.
- Gur, D., Leshem, B., Pierantoni, M., Farstey, V., Oron, D., Weiner, S. and Addadi, L. (2015a). Structural basis for the brilliant colors of the sapphirinid copepods. *J. Am. Chem. Soc.* **137**, 8408–8411.
- Gur, D., Palmer, B. A., Leshem, B., Oron, D., Fratzl, P., Weiner, S. and Addadi, L. (2015b). The mechanism of color change in the neon tetra fish: a light-induced tunable photonic crystal array. *Angew. Chem. Int. Ed. Engl.* **54**, 12426–12430.
- Hallberg, E. and Hagberg, M. (1986). Ocellar fine structure in *Caenis robusta* (Ephemeroptera), *Trichostegia minor*, *Agrypnia varia*, and *Limnephilus flavicornis* (Trichoptera). *Protoplasma* **135**, 12–18.
- Hamdorf, K., Höglund, G., Juse, A. and Stusek, P. (1989). Effect of neurotransmitters on movement of screening pigment in insect superposition eyes. *Z. Naturforsch.* **44c**, 992–998.
- Hanström, B. (1940). Inkretorische Organe, Sinnesorgane und Nervensystem des Kopfes einiger niederer Insektenordnungen. *Kungl. Svenska Vetenskapsakad. Handl.* **18**, 1–266.
- Hesse, R. (1901). Untersuchungen über die Organe der Lichtempfindung bei niederen Tieren. *Z. Wiss. Zool.* **70**, 347–473.
- Hirsch, A., Gur, D., Polishchuk, I., Levy, D., Pokroy, B., Cruz-Cabeza, A. J., Addadi, L., Kronik, L. and Leiserowitz, L. (2015). "Guanigma": the revised structure of biogenic anhydrous guanine. *Chem. Materials* **27**, 8289–8297.
- Homann, H. (1924). Zum Problem der Ocellenfunktion bei den Insekten. *Z. vergl. Physiol.* **1**, 541–578.
- Horridge, G. A. (ed) (1975). *The Compound Eye and Vision of Insects*. Oxford: Clarendon Press.
- Hsiung, B.-K., Blackledge, T. A. and Shawkey, M. D. (2015). Spiders do have melanin after all. *J. Exp. Biol.* **218**, 3632–3635.
- Insausti, T. C. and Casas, J. (2008). The functional morphology of color changing in a spider: development of ommochrome pigment granules. *J. Exp. Biol.* **211**, 780–789.
- Insausti, T. C. and Lazzari, C. R. (2002). The fine structure of the ocelli of *Triatoma infestans* (Hemiptera: Reduviidae). *Tissue Cell* **34**, 437–449.
- Iwasaka, M., Mizukawa, Y. and Roberts, N. W. (2016). Magnetic control of the light reflection anisotropy in a biogenic guanine microcrystal platelet. *Langmuir* **32**, 180–187.
- Jordan, T. M., Partridge, J. C. and Roberts, N. W. (2012). Non-polarizing broadband multilayer reflectors in fish. *Nat. Photonics* **6**, 759–763.
- Jordan, T. M., Partridge, J. C. and Roberts, N. W. (2014). Disordered animal multilayer reflectors and the localization of light. *J. R. Soc. Interface* **11**, 20140948.
- Kanehisa, M., Goto, S., Sato, Y., Kawashima, M., Furumichi, M. and Tanabe, M. (2014). Data, information, knowledge and principle: back to metabolism in KEGG. *Nucleic Acids Res.* **42**, D199–D205.
- King, C. A. and Cronin, T. W. (1994a). Investigations of pigment granule transport systems in *Gonodactylus oerstedii* (Crustacea: Hoplocarida: Stomatopoda) I. Effects of low temperature on the pupillary response. *J. Comp. Physiol. A* **175**, 323–329.
- King, C. A. and Cronin, T. W. (1994b). Investigations of pigment granule transport systems in *Gonodactylus oerstedii* (Crustacea: Hoplocarida: Stomatopoda) II. Effects of low temperature on pigment granule position and microtubule populations in reticular cells. *J. Comp. Physiol. A* **175**, 331–342.
- Kleinholz, L. H. (1959). Purines and pteridines from the reflecting pigment of the arthropod retina. *Biol. Bull.* **116**, 125–135.
- Klown, M. J. (2013). *Physiological Systems in Insects*. San Diego: Academic Press.
- Krapp, H. G. (2009). Ocelli. *Curr. Biol.* **19**, R435–R437.
- Lancaster, J. and Downes, B. J. (2013). *Aquatic Entomology*. Oxford: Oxford University Press.
- Land, M. F. (1972). The physics and biology of animal reflectors. *Prog. Biophys. Mol. Biol.* **24**, 75–106.
- Land, M. F. (1981). Optics and vision in invertebrates. In *Comparative Physiology and Evolution of Vision in Invertebrates. B: Invertebrate Visual Centers and Behavior I*, Vol. VII/6B of Handbook of Sensory Physiology (ed. H. Autrum), pp. 472–592. Berlin: Springer.
- Land, M. F. and Nilsson, D.-E. (2012). *Animal Eyes*. Oxford: Oxford University Press.
- Lazzari, C. R., Fischbein, D. and Insausti, T. C. (2011). Differential control of light-dark adaptation in the ocelli and compound eyes of *Triatoma infestans*. *J. Insect Physiol.* **57**, 1545–1552.
- Levy-Lior, A., Pokroy, B., Levavi-Sivan, B., Leiserowitz, L., Weiner, S. and Addadi, L. (2008). Biogenic guanine crystals from the skin of fish may be designed to enhance light reflectance. *Crystal Growth Design* **8**, 507–511.
- Meyer-Arendt, J. R. (1995). *Introduction to Classical and Modern Optics*. Englewood Cliffs, NJ: Prentice Hall.
- Meyer-Rochow, V. B. (1999). Photoreceptor ultrastructure in the Antarctic mussel shrimp *Acetabulastoma* (Crustacea: Ostracoda), a parasite of *Glyptonotus antarcticus* (Crustacea: Isopoda). *Polar Biol.* **21**, 166–170.
- Miller, W. (1979). Ocular optical filtering. In *Comparative Physiology and Evolution of Vision in Invertebrates. A: Invertebrate Photoreceptors*, Vol. VII/6A of Handbook of Sensory Physiology (ed. H. Autrum), pp. 69–143. Berlin: Springer.
- Misof, B., Liu, S., Meusemann, K., Peters, R. S., Donath, A., Mayer, C., Frandsen, P. B., Ware, J., Flouri, T., Beutel, R. G. et al. (2014). Phylogenomics resolves the timing and pattern of insect evolution. *Science* **346**, 763–767.
- Mizunami, M. (1995). Functional diversity of neural organization in insect ocellar systems. *Vision Res.* **35**, 443–452.
- Mizuno, H., Fujiwara, T. and Tomita, K.-I. (1969). The crystal and molecular structure of the sodium salt of xanthine. *Bull. Chem. Soc. Jpn.* **42**, 3099–3105.
- Mueller, K. P. and Labhart, T. (2010). Polarizing optics in a spider eye. *J. Comp. Physiol. A* **196**, 335–348.
- Nakakoshi, M., Nishioka, H. and Ktayama, E. (2011). New versatile staining reagents for biological transmission electron microscopy that substitute for uranyl acetate. *J. Electron Microsc.* **60**, 401–407.
- Nordström, M. and Warrant, E. J. (2000). Temperature-induced pupil movements in insect superposition eyes. *J. Exp. Biol.* **203**, 685–692.
- Oaki, Y., Kaneko, S. and Imai, H. (2012). Morphology and orientation control of guanine crystals: a biogenic architecture and its structure mimetics. *J. Mater. Chem.* **22**, 22686.

- Olivo, R. F. and Chrismer, K. L.** (1980). Spectral sensitivity of screening-pigment migration in retinula cells of the crayfish *Procambarus*. *Vision Res.* **20**, 385–389.
- O'Neil, M.**, ed. (2006). *The Merck Index: An Encyclopedia of Chemicals, Drugs, and Biologicals*, 14 edn. Whitehouse Station, NJ: Merck Research Laboratories.
- Paulus, H. F.** (1972). Die Feinstruktur der Stirnagen einiger Collembolen (Insecta, Entognatha) und ihre Bedeutung für die Stammesgeschichte der Insekten. *Z. Zool. Syst. Evol.* **10**, 81–122.
- Raman, C. V. and Krishnan, K. S.** (1928). A new type of secondary radiation. *Nature* **121**, 501–502.
- Reimann, A. and Richter, S.** (2007). The nauplius eye complex in 'conchostracans' (Crustacea, Branchiopoda: Laevicaudata, Spinicaudata, Cyclestherida) and its phylogenetic implications. *Arthropod Struct. Dev.* **36**, 408–419.
- Ribi, W. A. and Zeil, J.** (2015). The visual system of the Australian 'redeye' cicada (*Psaltoda moerens*). *Arthropod Struct. Dev.* **44**, 574–586.
- Ribi, W., Warrant, E. and Zeil, J.** (2011). The organization of honeybee ocelli: regional specializations and rhabdom arrangements. *Arthropod Struct. Dev.* **40**, 509–520.
- Rieger, D., Stanewsky, R. and Helfrich-Förster, C.** (2003). Cryptochrome, compound eyes, Hofbauer-Buchner eyelets, and ocelli play different roles in the entrainment and masking pathway of the locomotor activity rhythm in the fruit fly *Drosophila melanogaster*. *J. Biol. Rhythms* **18**, 377–391.
- Ruck, P. and Edwards, G.** (1964). The structure of the insect dorsal ocellus. I. General organization of the ocellus in dragonflies. *J. Morph.* **115**, 1–26.
- Saenko, S. V., Teyssier, J., van der Marel, D. and Milinkovitch, M. C.** (2013). Precise colocalization of interacting structural and pigmentary elements generates extensive color pattern variation in *Phelsuma* lizards. *BMC Biol.* **11**, 105.
- Saunders, D.** (1976). *Insect Clocks*. Oxford: Pergamon Press.
- Schindelin, J., Arganda-Carreras, I., Frise, E., Kaynig, V., Longair, M., Pietzsch, T., Preibisch, S., Rueden, C., Saalfeld, S., Schmid, B. et al.** (2012). Fiji: an open-source platform for biological-image analysis. *Nat. Methods* **9**, 676–682.
- Schuppe, H. and Hengstenberg, R.** (1993). Optical properties of the ocelli of *Calliphora erythrocephala* and their role in the dorsal light response. *J. Comp. Physiol. A* **173**, 143–149.
- Schwab, I. R., Carlton, K., Buyukmihci, N., Blankenship, T. and Fitzgerald, P.** (2002). Evolution of the tapetum. *Trans. Am. Ophthalmol. Soc.* **100**, 187–202.
- Schwarz, S., Albert, L., Wystrach, A. and Cheng, K.** (2011a). Ocelli contribute to the encoding of celestial compass information in the Australian desert ant *Melophorus bagoti*. *J. Exp. Biol.* **214**, 901–906.
- Schwarz, S., Wystrach, A. and Cheng, K.** (2011b). A new navigational mechanism mediated by ant ocelli. *Biol. Lett.* **7**, 856–858.
- Somanathan, H., Kelber, A., Borges, R. M., Wallén, R. and Warrant, E. J.** (2009). Visual ecology of Indian carpenter bees II: adaptations of eyes and ocelli to nocturnal and diurnal lifestyles. *J. Comp. Physiol. A* **195**, 571–583.
- Speiser, D. I. and Johnsen, S.** (2008). Comparative morphology of the concave mirror eyes of scallops (Pectinoidea). *Am. Malac. Bull.* **26**, 27–33.
- Stange, G., Stowe, S., Chahl, J. S. and Massaro, A.** (2002). Anisotropic imaging in the dragonfly median ocellus: a matched filter for horizon detection. *J. Comp. Physiol. A Sens. Neural Behav. Physiol.* **188**, 455–467.
- Stavenga, D. G.** (1979). Pseudopupils of compound eyes. In *Comparative Physiology and Evolution of Vision in Invertebrates. A: Invertebrate Photoreceptors*, Vol. VII/6A of Handbook of Sensory Physiology (ed. H. Autrum), pp. 357–439. Berlin: Springer.
- Stavenga, D. G., Bernard, G. D., Chappell, R. L. and Wilson, M.** (1979). Insect pupil mechanisms. III. On the pigment migration in dragonfly ocelli. *J. Comp. Physiol. A* **129**, 199–205.
- Strausfeld, N. J.** (2005). The evolution of crustacean and insect optic lobes and the origins of chiasmata. *Arthropod Struct. Dev.* **34**, 235–256.
- Sturm, H.** (1997). A new subgenus and two new species of the genus *Machilinus* (Meinertellidae, Archaeognatha=Microcoryphia, "Apterygota", Insecta) from Mexico. *J. New York Ent. Soc.* **105**, 15–23.
- Sturm, H. and Machida, R.** (2001). *Archaeognatha*, Vol. 4 of Handbuch der Zoologie. Berlin: Walter de Gruyter.
- Sturm, H. and Smith, G. B.** (1993). New bristle tails (Archaeognatha: Meinertellidae) from Australia. *J. Aust. Ent. Soc.* **32**, 233–240.
- Taylor, G. K. and Krapp, H. G.** (2007). Sensory systems and flight stability: what do insects measure and why? In *Insect Mechanics and Control*, Vol. 34 of Advances in Insect Physiology (ed. J. Casas and S. Simpson), pp. 231–316. San Diego: Academic Press.
- Teyssier, J., Saenko, S. V., van der Marel, D. and Milinkovitch, M. C.** (2015). Photonic crystals cause active colour change in chameleons. *Nat. Commun.* **6**, 6368.
- Toh, Y. and Sagara, H.** (1984). Dorsal ocellar system of the American cockroach: I. Structure of the ocellus and ocellar nerve. *J. Ultrastruct. Res.* **86**, 119–134.
- Tomioka, K. and Abdelsalam, S.** (2004). Circadian organization in hemimetabolous insects. *Zool. Sci.* **21**, 1153–1162.
- van Kleef, J., James, A. C. and Stange, G.** (2005). A spatiotemporal white noise analysis of photoreceptor responses to UV and green light in the dragonfly median ocellus. *J. Gen. Physiol.* **126**, 481–497.
- Warrant, E. J.** (2006). *Invertebrate vision*. Cambridge: Cambridge University Press.
- Warrant, E. J. and Nilsson, D.-E.** (1998). Absorption of white light in photoreceptors. *Vision Res.* **38**, 195–207.
- Waterman, T.** (1981). Polarization sensitivity. In *Comparative Physiology and Evolution of Vision in Invertebrates. B: Invertebrate Visual Centers and Behavior I*, Vol. VII/6B of Handbook of Sensory Physiology (ed. H. Autrum), pp. 281–469. Berlin: Springer.
- Wilson, M.** (1975). Autonomous pigment movement in the radial pupil of locust ocelli. *Nature* **258**, 603–604.
- Wilson, M.** (1978). The functional organisation of locust ocelli. *J. Comp. Physiol. A* **124**, 297–316.
- Wygodzinsky, P. W.** (1941). Beiträge zur Kenntnis der Dipluren und Thysanuren der Schweiz. *Denkschr. Schweiz. Naturf. Ges.* **74**, 107–227.
- Yanoviak, S. P., Kaspary, M. and Dudley, R.** (2009). Gliding hexapods and the origins of insect aerial behaviour. *Biol. Lett.* **5**, 510–512.
- Zeil, J., Ribi, W. A. and Narendra, A.** (2014). Polarisation vision in ants, bees and wasps. In *Polarized Light and Polarization Vision in Animal Sciences* (ed. G. Horváth), pp. 41–60. Berlin: Springer.
- Zyznar, E. S. and Nicol, J. A. C.** (1971). Ocular reflecting pigments of some Malacostraca. *J. Exp. Mar. Biol. Ecol.* **6**, 235–248.

Supplementary files



Movie 1: Pigment migration during light adaptation in the lateral ocellus of *Machilis hrabei* and *Lepismachilis notata*. Medial to the right, dorsal up. Playback speed 60x, real duration: 30 minutes.

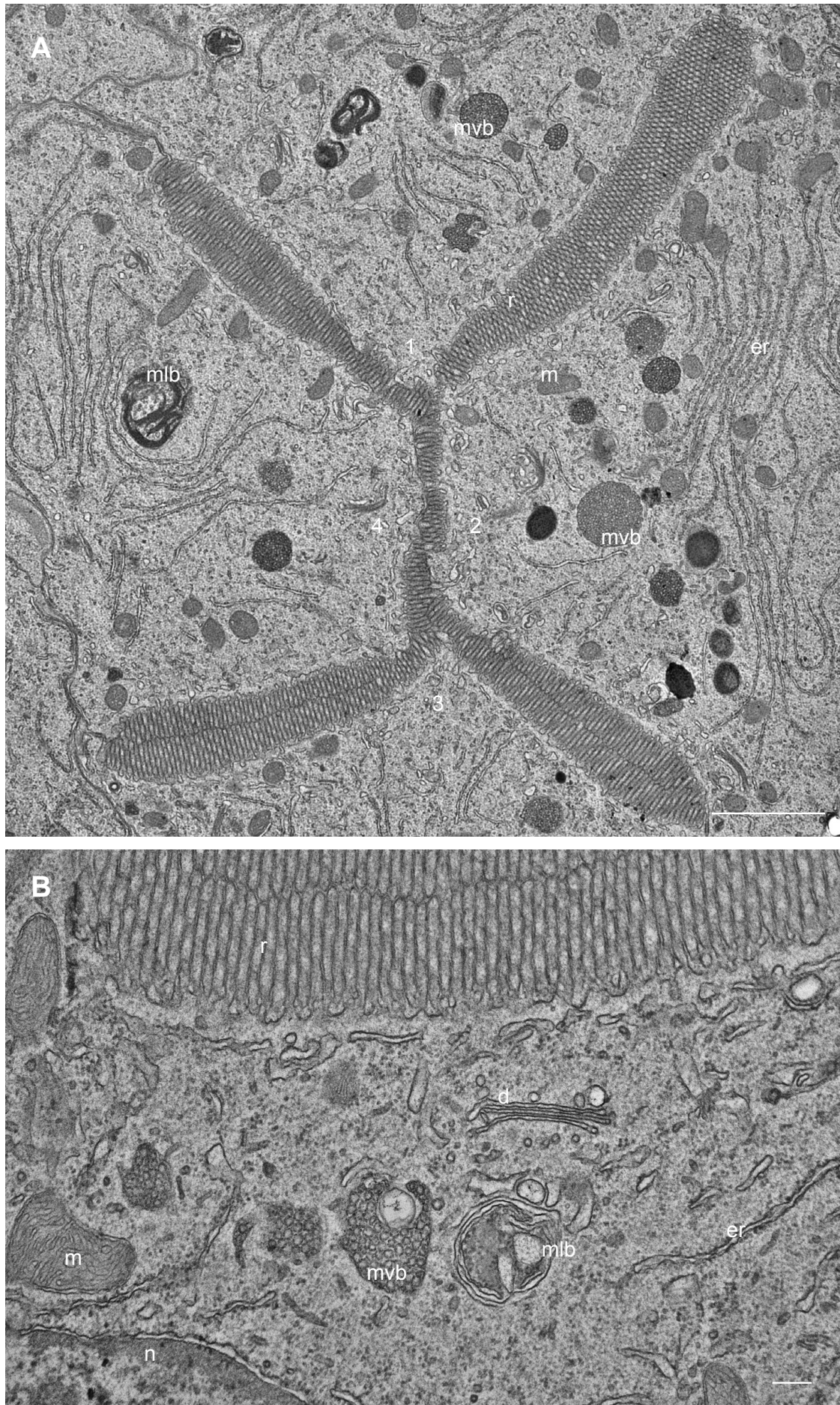


Fig. S1: Ultrastructural detail of photoreceptor cells in a dark adapted *Machilis hrabei* lateral ocellus. Numbers in A denote the four receptor cells. Abbreviations: d dictyosome, er rough endoplasmic reticulum, m mitochondrion, mlb multilamellar body, mvb multivesicular body, n nucleus, r rhabdom. Scale bars: A 2000 nm, B 200 nm.